Inhibitory Effects of HangAmDan-B1 (HAD-B1) Combined With Afatinib on H1975 Lung Cancer Cell–Bearing Mice

Hwa Jeong Kang, MS[1],[*], Jeehye Kim, MS[2],[*], Seong Hyeok Cho, MS[1],
So-Jung Park, OMD[2], Hwa-Seung Yoo, OMD[2], and In-Cheol Kang, PhD[1],[3]

Abstract

Epidermal growth factor receptor mutation-positive non–small cell lung cancer is cared for mainly by target therapeutics in the clinical treatment at present. We investigated the antitumor effect of HangAmDan-B1 (HAD-B1) combined with afatinib on H1975 (L858R/T790M double mutation) lung cancer cells. The combined treatment of HAD-B1 with afatinib inhibited the proliferation of H1975 cells in a dose-dependent manner compared with the treatment of afatinib or HAD-B1 alone. The combined treatment group significantly induced early apoptosis and cell cycle arrest of the cells compared with afatinib- or HAD-B1-treated control group. Profile analysis of cell cycle proteins in H1975 cells treated with the combination of HAD-B1 and afatinib using InnoPharmaScreen antibody microarray showed downregulation of pERK1/2 and upregulation of p16 in the cells. In vivo tumor growth assay in xenograft animal model of human H1975 lung cancer cells revealed that the mean tumor volume in the group treated with the combination of HAD-B1 and afatinib showed a significant reduction compared with the control groups.

Keywords

HangAmDan-B1, H1975 cells, EGFR L858R/T790M double mutation cells, lung cancer

Introduction

Lung cancer is the most common malignancy worldwide and is ranked as the first cause of cancer-related mortality for both men and women.[1] Non–small cell lung cancer (NSCLC) accounts for up to 85% of all lung cancers and more than 40% of NSCLC patients are diagnosed with metastatic (Stage IV) disease.[2] In the past decade, the landscape of advanced NSCLC therapies has been rapidly evolving beyond chemotherapy with the discovery of oncogenic driver mutations.[3] Somatic epidermal growth factor receptor (EGFR) mutations are present in approximately 50% of patients in Asia and in 10% to 15% of Caucasian patients with metastatic NSCLC.[4] Most of these mutations are caused by deletion on the exon 19 or L858R point mutations on exon 21.[5] EGFR tyrosine kinase inhibitors (TKIs) such as erlotinib, gefitinib, and afatinib have demonstrated an improved tumor response rate and prolonged progression-free survival compared with standard chemotherapy.[6] However, despite an initial dramatic response to EGFR-TKIs, acquired resistance usually occurred when patients were treated with EGFR inhibitors for 10 to 14 months.[7]

Much evidence identified that more than 50% of the EGFR-TKI resistance is caused by a T790M point mutation in the catalytic cleft of the EGFR tyrosine kinase domain.[8] Afatinib is an irreversible second-generation EGFR-TKI that inhibits all ErbB family members by forming covalent bonds to the receptors.[9] Its irreversible inhibition could be potentially effective in inhibiting EGFR T790M-derived signaling pathway and provide more improved clinical benefit than the reversible first-generation EGFR-TKIs.[9-12] However, acquired resistance also occurred when patients were treated with afatinib as first-line therapy,[13] and adverse

[1]Hoseo University, Asan, Chungcheongnam-do, Republic of Korea
[2]Dunsan Oriental Medical Hospital of Daejeon University, Daejeon, Chungcheongnam-do, Republic of Korea
[3]InnoPharmaScreen Inc, Asan, Chungcheongnam-do, Republic of Korea

[*]These authors equally contributed to this work.

Corresponding Author:
In-Cheol Kang, Department of Biological Science and BioChip Research Center, Hoseo University, 20, Hoseo-ro79beon-gil, Baebang-eup, Asan, Chungcheongnam-do 336-795, Republic of Korea.
Email: ickang@hoseo.edu

Table 1. Ingredients of HangAmDan-B1 (HAD-B1).[20]

Scientific Name	Relative Amount
Panax Notoginseng Radix	25.2 (32.3)
Cordyceps militaris	19.2 (24.6)
Panax ginseng CA Meyer	19.2 (24.6)
Boswellia carterii Birdwood	14.4 (18.5)
Total amount	78.0 (100)

effects such as rash and diarrhea of grade ≥3 were significantly more frequent with afatinib therapy than with erlotinib or gefitinib therapy.[14] Therefore, it is necessary to discover adjuvant natural product drugs that have few side effects and high efficiency against NSCLC on account of the shortcomings of current drugs to overcome EGFR-TKI resistance and prolong the survival of patients with NSCLC. HangAmDan-B1 (HAD-B1), the upgraded version of HangAmDan-B (HAD-B), is used as an anticancer medication at the East West Cancer Center (EWCC; Dunsan Korean Medicine Hospital, Daejeon University, Korea). Several studies supported the anticancer effect of HAD-B in various cancer cells including human NSCLC cells.[15-19] HAD-B1, a herbal aqueous extract, composed of 4 critical herbs (Panax Notoginseng Radix, *Cordyceps militaris, Panax ginseng* CA Mey, and *Boswellia carteri* Birdw), was developed to focus on lung cancer treatment. This study was conducted to investigate the anticancer effects of the HAD-B1 combined with afatinib on H1975 EGFR-L858R/T790M double mutation lung cancer cells with the biological mechanism and solid tumor growth in nude mice bearing a H1975 human lung cancer xenograft.

Materials and Methods

Preparation of HAD-B1 Extract

HAD-B1 was provided by the EWCC. A voucher specimen (#HAD-B-1-2014-10-HS) has been deposited at the Institute of Traditional Medicine and Bioscience in Daejeon University. The ingredients of the herb mixture (HAD-B1) were soaked for 18 hours in a soaking bath at 60°C of distilled water (DW) and the supernatant was obtained. The extracts were concentrated by using a rotary vacuum evaporator at 60°C for 2 hours and were dried on a flat evaporator at 60°C for 8 hours, and the powder produced was used for the experiments (Table 1).[20] The HAD-B1 was dissolved in DW.

High-Performance Liquid Chromatography (HPLC) Analysis of HAD-B1

The HAD-B1 stock was prepared by extracting HAD-B1 powder with 1 mg of powder in 10 mL of DW at room temperature. The extract was then centrifuged at $1000 \times g$ for 30 minutes and filtered and applied to the C18 column and

eluted using acetonitrile mixed with DW. Figure 1 shows the results of HPLC of HAD-B1 fractions.

Cell Culture

H1975 (EGFR-L858R/T790M double mutation human lung cancer) cells were cultured in RPMI1640 containing 10% fetal bovine serum and 1X antibiotics (Welgene, Daejeon, Korea). The H1975 cells cultures were maintained at 37°C in a humidified atmosphere with 5% CO_2.

In Vitro H1975 Cell Proliferation Assay

H1975 cells (2×10^3 cells/well) were added to 96-well tissue culture plates coated with gelatin and allowed to adhere overnight. The cells were treated with HAD-B1 and afatinib that had been incubated for 72 hours. Then, 50 μL of a 1 mg/mL MTT solution was added to each well, and the cells were incubated for 2 hours at 37°C. After the supernatants had been discarded, the residual formazan crystals were dissolved in 100 μL of dimethyl sulfoxide. The absorbance was measured at 595 nm on an ELISA plate reader (EMax, Molecular Devices, San Jones, CA). The measurements were made in triplicate.

Annexin V/Dead Cell and Cell Cycle Analysis

The H1975 cells were treated with HAD-B1 for 24 hours and 48 hours, respectively. Cell viability and apoptosis were determined using the MUSE Annexin V and dead cell kit in accordance to the recommended protocol. Cell cycle analysis was measured with Muse cell cycle kit (Merck Millipore, Billerica, MA).

Caspase Activity Assay

The H1975 cells were collected by using trypsin-ethylenediaminetetraacetic acid (EDTA) after incubation with HAD-B1 and afatinib for 72 hours. Collected cells were centrifuged, the supernatant was discarded, and the remaining cell pellet was incubated with lysis-M solution on ice for 15 minutes. After incubation, the lysed cells were centrifuged, and the amount of protein in the supernatant was quantified. Protein, 100 μg/50 μL, was added into the wells in the 96-well plate, and a 1 M DTT (dithiothreitol) dilution was used to reach the final concentration of 0.1 M in each well. Then, 5 μL of LEHD-pNA was added to each well, and the plate was incubated at 37°C for 2 hours. The absorbance was measured at 405 nm by using a microplate reader.

Protein Extraction From H1975 Cells and the Fluorescence Labeling

H1975 cells were serum-starved by incubation in RPMI1640 for 4 hours. The cells were treated with or without HAD-B1.
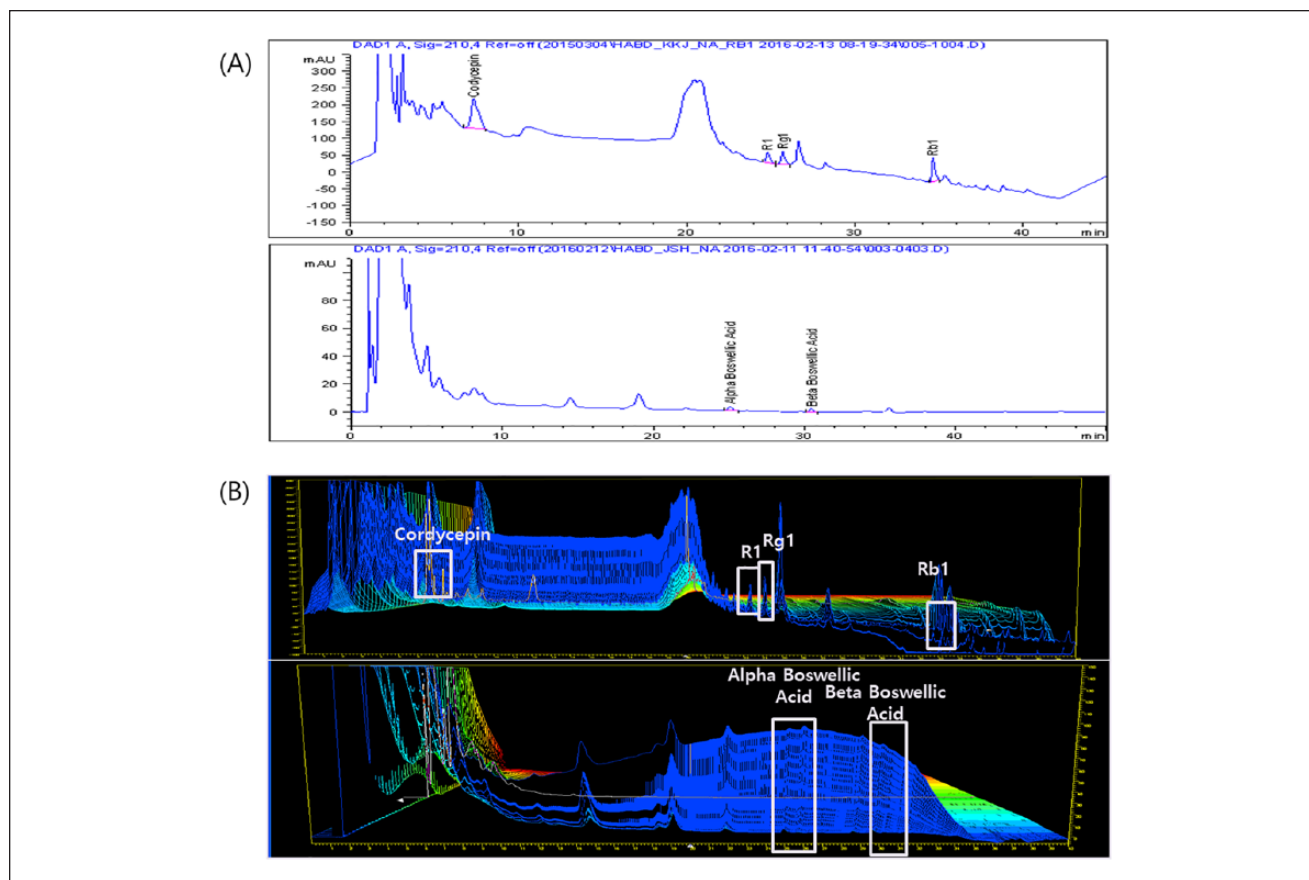
Figure 1. HPLC profile of major components in HAD-B1. For the quantitative analysis of 1 tablet of HAD-B1, methanol extract of HAD-B1 was applied to the octadecylsilylated silica gel column on HPLC and eluted by acetonitrile mixed with distilled water (A). The 3-dimensional HPLC profile of HAD-B1 (B). HAD-B1 detected the presence of 6 compounds: cordycepin, R1, Rg1, Rb1, α-boswellic acid, and β-boswellic acid.

After 72 hours incubation, the cells were washed twice with phosphate-buffer saline (PBS) and harvested in 5-mM trypsin-EDTA. The harvested cells were centrifuged for 15 minutes at 1800 rpm. The pellets were washed with PBS and recentrifuged. H1975 cells were extracted with Lysis-M (Roche, Mannheim, Germany) mammalian cell extraction buffer. Each protein extract (100 mg, 1 mg/mL) was labeled with both Cyanine3 and Cyanine5 (GE Healthcare, Buckinghamshire, UK) as per the manufacturer's instructions. Free dyes were removed with Sigma Spin columns (S5059, Sigma, St Louis, USA) and purified samples were stored at 4°C until use.

Preparation of InnoPharmaScreen (IPS)-Forward Phase Antibody Array (FPAA)

Forty-two distinct antibodies against the proteins involved in cell proliferation were spotted onto IPS antibody arrays in duplicate (Figure 3C). The detailed procedure for the array analysis has been described elsewhere.[17]

Profile Analysis of Cell Cycle Proteins Using IPS-FPAA

The fluorescence-labeled cell lysates were applied to the antibody array and incubated for 1 hour at 37°C in the dark. The slides were washed 3 times with phosphate-buffered saline with tween (PBST), dried with N_2, and analyzed by using a fluorescence microarray scanner. The antibody array slides were scanned by using a GenePix 4100A microarray scanner (Axon Instruments, Union City, CA) with 532- and 635-nm lasers. Image analysis was performed for each spot by using the manufacturer's software package (GenePix 6.0, Axon Instruments). The internally normalized ratios of all spots were calculated by using a procedure that is described elsewhere.[21]

Western-Blot Analysis

H1975 cells were incubated with HAD-B1 and with afatinib in RPMI1640 (2% fetal bovine serum, 1× antibiotics)

for 72 hours, after which the cells were harvested to extract the proteins. The cell lysates were prepared in Lysis-M buffer (Roche) containing protease and phosphatase inhibitor cocktails (both from Roche). The cell lysates were clarified by centrifugation. Lysates containing 30 μg of protein were loaded into each well and separated through 12% sodium dodecyl sulfate–gel electrophoresis. Gels were soaked in transfer buffer (16 mM Tris-HCl, 30-mM glycine, and 20% methanol), and proteins were then transferred to polyvinylidene difluoride membranes. Nonspecific binding sites were blocked by incubation with 5% nonfat dry milk in PBST (137 mM NaCl, 27 mM KCl, 100 mM Na_2HPO_4, 20 mM KH_2PO_4, 0.05% Tween20, and pH 7.4). The polyvinylidene difluoride membranes were then incubated with primary antibodies against p-ERK1/2 (1:1000), ERK1/2 (1:1000), p-EGFR (1:1000), EGFR (1:1000), p16 (1:1000), and β-actin (1:10000) in PBST containing 5% bovine serum albumin and 5% nonfat dry milk at 4°C overnight. Membranes were washed with PBST and incubated with secondary antibodies (anti-mouse at 1:16 000, anti-rabbit at 1:16 000). Signals were then developed by using an enhanced chemiluminescence Western blotting detection kit and were exposed to X-ray films.

In Vivo Tumor Growth Assay in Xenograft Animal Model of Human H1975 Lung Cancer Cells

H1975 cells were injected subcutaneously to generate a xenograft model in mice. Once the tumor size reached 100 mm^3, HAD-B1 and afatinib were administered orally once daily for 30 days, during which time the tumor size and body weight were checked daily. Blood biochemical tests were carried out using an automatic biochemical analyzer (HITACHI, Tokyo, Japan). All care and handling of the animals were performed according to the *Guide for the Care and Use of Laboratory Animals* (HTRC-16-37(1)).

Statistical Analysis

All data are expressed as the mean ± standard deviation, and statistical comparisons were performed using a Student's *t* test. Caspase activity data were compared using 1-way analysis of variance with post hoc Dunnett's test. Statistical analyses were performed using Microsoft Office Excel version 2007 (Microsoft Corporation, Redmond, WA). *P* < .05 was considered to indicate a statistically significant difference.

The combination index (CI) is widely used to quantify drug synergism based on the multiple drug effect equation of Chou-Talalay.[22,23] The CI values were determined for each concentration of afatinib, HAD-B1, and their combination in

Table 2. Combination Index (CI) Analysis of HAD-B1 Combined With Afatinib at a Nonconstant Ratio in H1975 Cells[a].

HAD-B1 (mg/mL)	Combination Index[b]
20	1.1
5	0.47
1.25	1.07
0.31	0.04
0.078	0.11

[a]Data are values from Figure 2.
[b]CI = 1.00, additive; CI < 1.00, synergistic; CI > 1.00, antagonistic.

cell proliferation assays using CompuSyn (ComboSyn, Inc, Paramus, NJ; Table 2). CI < 0.9 indicates synergism, CI = 0.9 to 1.10 indicates additive interaction, and CI > 1.10 indicates antagonism.[22]

Results

Profiling of Major Components in HAD-B1 Using on HPLC Analysis

HAD-B1 is an anticancer medication developed to focus on lung cancer treatment. It is composed of 4 herbs that have positive effects on lung cancer. The 3-dimensional HPLC analysis of HAD-B1 showed the presence of 6 critical compounds including cordycepin, R1, Rg1, Rb1, α-boswellic acid, and β-boswellic acid (Figure 1).

Inhibition of H1975 Cell Viability by HAD-B1

To examine the synergistic antiproliferative effects of combined treatment with HAD-B1 and afatinib on H1975 cells, we employed H1975 cell viability assay using MTT assay. The combination of HAD-B1 and afatinib inhibited the viability of H1975 cells in a dose-dependent manner. Half-maximal inhibition of H1975 cell viability by the combined treatment was observed at a concentration of 0.05 M and 0.03 ± 0.02 mg/mL (*P* < .05, .01; Figure 2C) whereas the IC50 values of afatinib or HAD-B1 alone were 0.057 ± 0.015 mM (Figure 2A) or 0.128 ± 0.064 mg/mL (Figure 2B), respectively. Cordycepin, one of the major components of HAD-B1, also inhibited the viability of H1975 cells and half-maximal inhibition of H1975 cell viability by cordycepin was observed at a concentration of 0.021 ± 0.006 mg/mL (*P* < .05, .01) but R1 and Rb1 showed no effects (Figure 2D). The CI values showed the synergistic effect of the combined treatment of HAD-B1 with afatinib (COMTHA) in the cell proliferation data (Table 2). These data demonstrated that HAD-B1 appeared to be synergistically effective in suppressing the cell viability by the combined administration of afatinib.
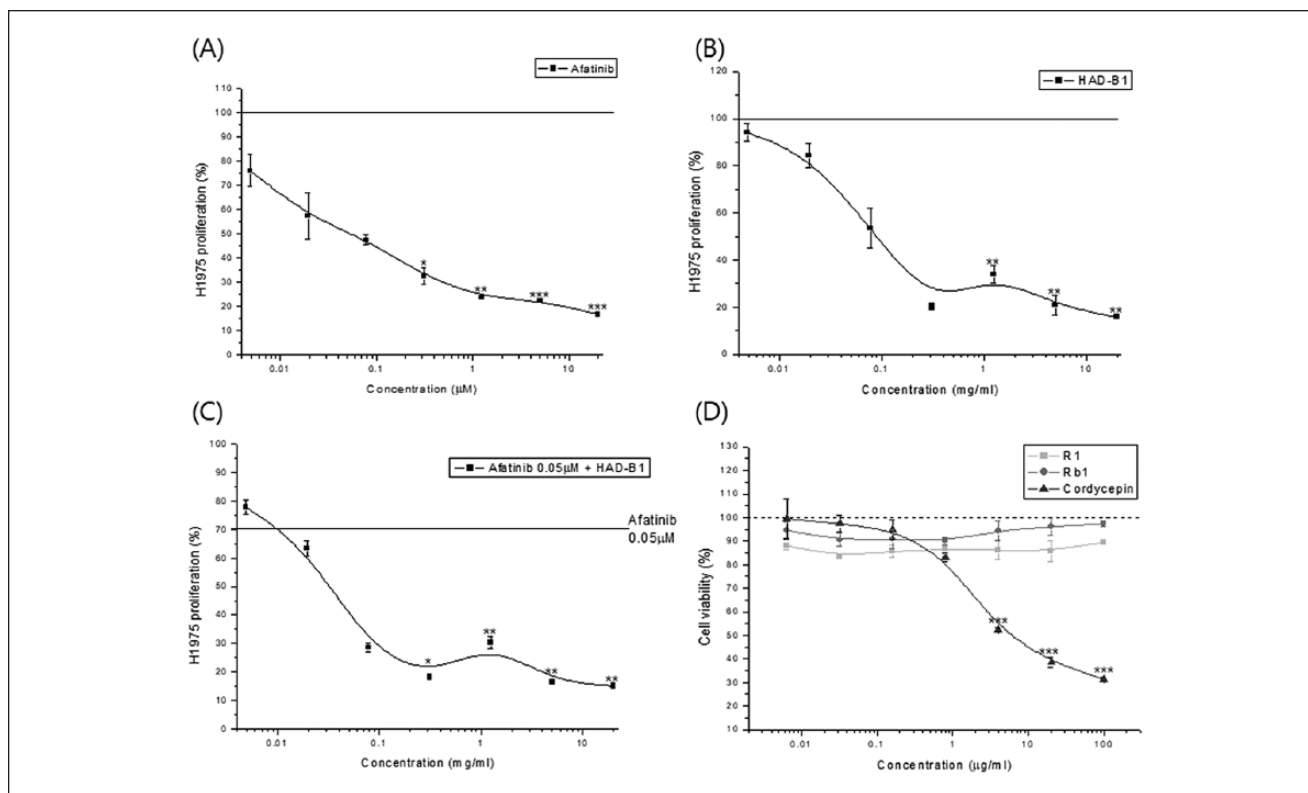
Figure 2. Cell-based viability assay using H1975 lung cancer cells treated with HAD-B1 in combination with afatinib. H1975 cells incubated with different concentrations of afatinib (A); HAD-B1 (B); combined treatment with afatinib (50 nM) and HAD-B1 (C); and cordycepin, a major compound of HAD-B1 (D) for 72 hours. Data shown are the means ± SD, and statistical analysis was performed using the Student's t test (n = 3; *P < .05, **P < .01, and ***P < .001, vs control).

Expression Profiling of Cell Cycle Proteins in H1975 Cells Treated With the Combination of HAD-B1 and Afatinib Using IPS FPAA

To investigate the molecular mechanism of the antiproliferative effect of HAD-B1 on H1975 cells, we performed the proteomic analysis of endogenous cell signaling proteins in H1975 cells treated with HAD-B1, using protein chip–based antibody microarray. Based on the data analysis, we found that HAD-B1 increased the expression of p16 (Figure 3E) whereas it decreased the expression of pERK1/2 protein (Figure 4). The expression data were validated by immunoblot analysis. These findings indicated that the inhibitory effect of HAD-B1 on H1975 cell proliferation was due to blocking ERK1/2-mediated cell survival signaling and enhancing p16.

Cell Cycle Analysis and Apoptosis Induction in H1975 Cells Treated With the COMTHA

To further investigate whether the inhibition of the cell survival by the treatment with HAD-B1 and afatinib on H1975 cell is closely related with the cell cycle arrest, we carried out cell cycle analysis using MUSE cell analyzer. The combined

treatment with HAD-B1 and afatinib was dosed in the cells for 24 hours and 48 hours, respectively. The cell apoptosis and cell cycle were analyzed using Muse cell cycle kit and Annexin V and dead cell kit. The early apoptosis rate was markedly increased in the COMTHA-treated cells compared with empty vehicle-treated control group (Figure 5), G0-G1 phase arrest (Figure 6) was increased in the COMTHA-treated cells.

Activation of Caspase-3, -8, and -9 in H1975 Cells Treated With the COMTHA

To confirm the induction of apoptosis in H1975 cells treated with the COMTHA, we carried out caspases (caspase-3, -8, and -9) activity assay in vitro. H1975 cells were treated with the COMTHA for 72 hours (Figure 7). Based on the results, the COMTHA appeared to be more effective in enhancing the caspase activities compared with afatinib alone.

Inhibitory Effect of the COMTHA on the Tumor Growth in H1975 Xenograft Mice

To further demonstrate the anti–lung cancer effect of the COMTHA in vivo, we conducted a solid tumor growth
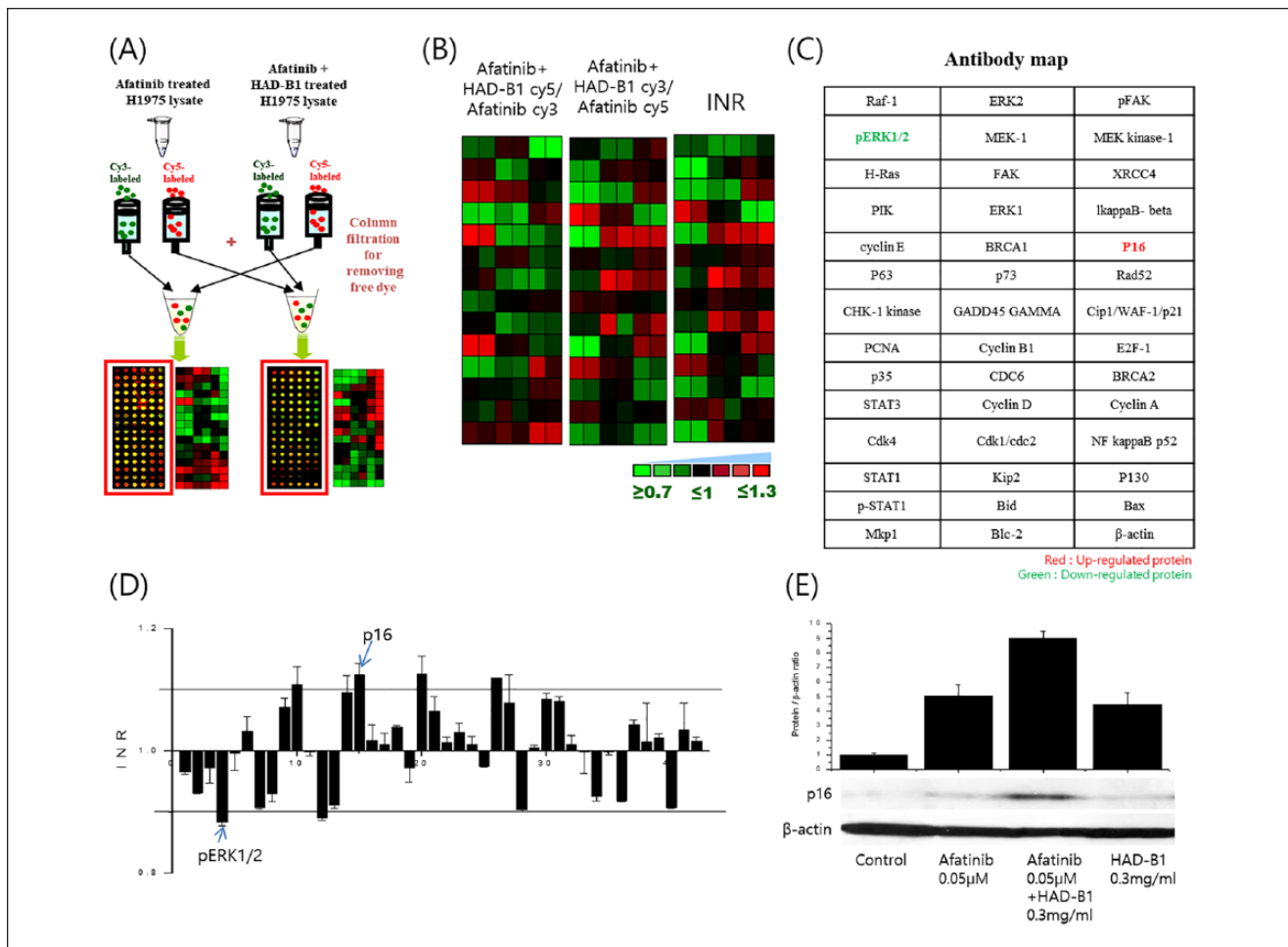
Figure 3. Differential expression profiling of cell cycle proteins in H1975 cells treated with the COMTHA using the IPS Forward Phase Antibody Array chip. Schematic diagram of protein expression profiling in H1975 cells treated with HangAmDan-B1 (HAD-B1) by using an antibody microarray on IPS Proteochip (A). Graded image of the Cy5:Cy3 ratios from the COMTHA-treated H1975 cells (B). Map of the antibody array chip (C). Graphical representation of the Cy5:Cy3 ratios on the antibody from H1975 cells treated with the COMTHA (D). Validation of the antibody microarray data based on an immune blot analysis (E).
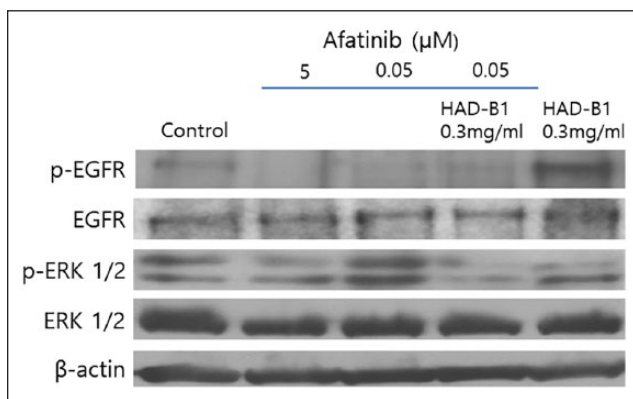

Figure 4. Inhibitory effect of epidermal growth factor receptor signaling in H1975 cells treated with the COMTHA. Western blot analysis of cell lysates from H1975 cells treated with the COMTHA for 24 hours.

assay using an H1975 cell–xenograft mouse model. Briefly, human lung cancer H1975 cells (1.0×10^6) were injected into the skin of nude mice and grown to a mass of approximately 100 mm³ (Figure 8B). The tumor growth was inhibited in a dose-dependent manner when the COMTHA combined treated was orally administered once daily to the mice. Moreover, the mean tumor volume in the group treated with the COMTHA (afatinib, 10 mg/kg; and HAD-B1, 400 mg/kg) was markedly reduced compared with those of the control groups treated with afatinib (10 mg/kg) alone (Figure 8A). Immunohistochemical analysis of the tumor tissues revealed downregulation of p-ERK and upregulation of p16 in COMTHA-treated group (Figure 8C and D). This result was consistent with the data of proteomic analysis in H1975 cells. Biochemical blood analysis of alanine aminotransferase, aspartate transaminase, alkaline phosphatase, blood urea nitrogen, and creatinine levels
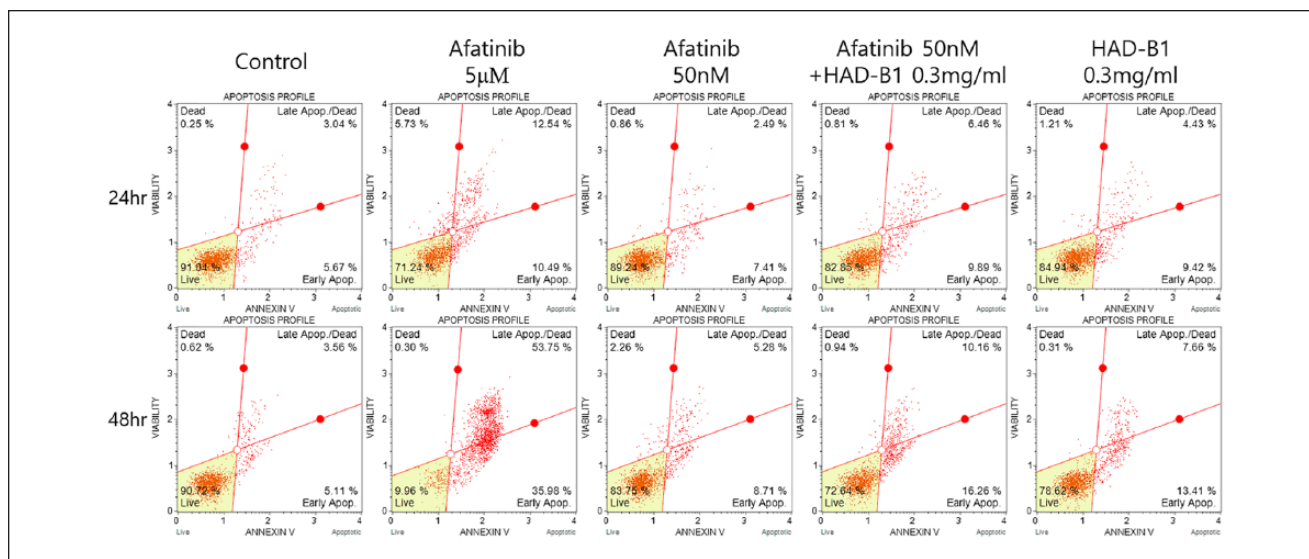
Figure 5. Apoptosis of H1975 cells treated with the COMTHA. The H1975 cells were treated with the COMTHA for 24 hours and 48 hours, respectively. Apoptosis was assessed by Annexin and 7-AAD double staining using Mini Flow Cytometry Muse Cell Analyzer.
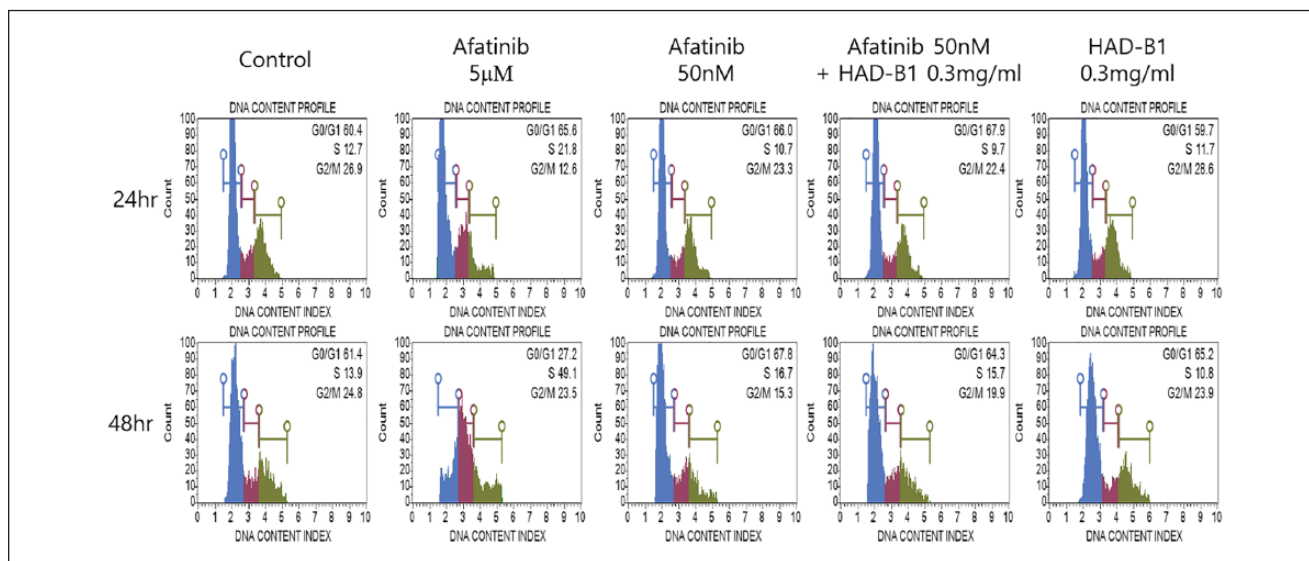

Figure 6. Cell cycle of H1975 cells treated with the COMTHA. H1975 cells were treated with the COMTHA for 24 hours and 48 hours, respectively. Cell cycle distribution was analyzed by Muse cell cycle kit (Merck Millipore, Billerica, MA).

did not reveal any significant changes in the COMTHA-treated group (Figure 9). These data demonstrated that HAD-B1 has potential for use as an inhibitor of solid tumor growth developed by H1975 lung cancer cells without any side effects.

Discussion and Conclusion

Afatinib showed activity in tumors resistant to first-generation EGFR-TKIs, including tumors harboring the EGFR L858R/T790M double mutant.[24] Nevertheless, application of afatinib brought about a high occurrence of adverse effects.[14] Therefore, it is necessary to discover natural product drugs that have few side effects and high efficiency against NSCLC on account of the shortcomings of current drugs in overcoming EGFR-TKIs resistance. HAD-B1 is an anticancer medication developed to focus on lung cancer treatment. It is composed of 4 herbs that have positive effects on lung cancer. The 3-dimensional HPLC analysis of HAD-B1 showed the presence of 6 critical compounds
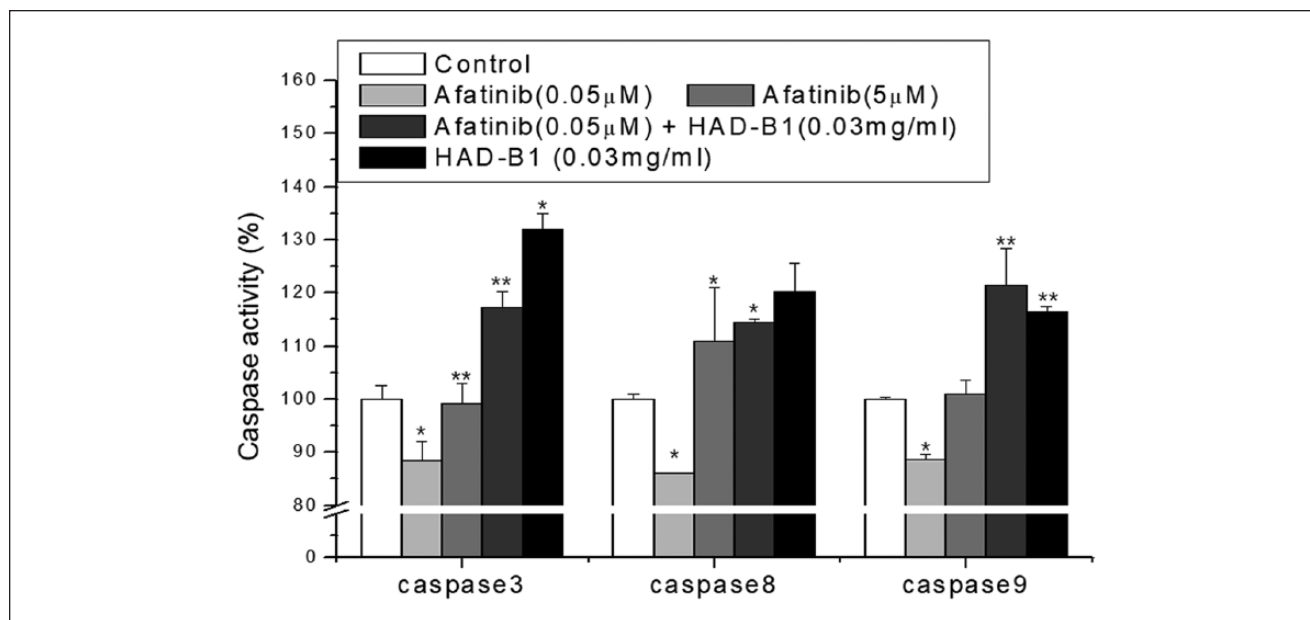
Figure 7. Analysis of caspase-3, -8, and -9 activities in H1975 cells treated with the COMTHA. The H1975 cells were treated with the COMTHA for 72 hours. The bar graph showed caspases activities compared with vehicle control as percentages. Afatinib was used as positive control. Data shown are the means ± SD, and statistical analysis was performed using 1-way analysis of variance with a post hoc Dunnett's test (n = 3; *P < .05, **P < .01, vs control).

including cordycepin, R1, Rg1, Rb1, α-boswellic acid, and β-boswellic acid (Figure 1). Cordycepin, an important compound from *Cordyceps militaris*, induces autophagy mediated c-FLIPL degradation and leads to apoptosis in human NSCLC cells.[25] Notoginsenoside R1 from *Panax notoginseng* suppresses cancer metastasis by inhibiting cell migration, invasion, and adhesion, and by regulating expression of metastasis-associated signaling molecules.[26] Major ginsenosides including Rg1, Rb1 from mountain ginseng induced apoptosis in lung cancer cells via extrinsic apoptotic pathway by increasing the expression of caspase-3 and caspase-8.[27] Boswellic acids from *Boswellia serrata* induced apoptosis through caspase activation, increased Bax expression, NF-κB downregulation, and induction of poly(ADP)-ribose polymerase cleavage.[28] In this study, we demonstrated anticancer effect by reducing the dose of afatinib and combining treatment with HAD-B1. In the in vitro H1975 cell viability assay, combined treatment with HAD-B1 and afatinib appeared to be more effective than afatinib or HAD-B1 alone (Figure 2). Also, cordycepin inhibited the viability of H1975 cells in a dose-dependent manner but R1 and Rb1 did not. These results suggest that cordycepin may significantly contribute to the antiproliferation effect on H1975 cells. One study reported that cordycepin induces apoptosis and inhibits proliferation of human H1975 lung cancer cell.[29] Proteomic analysis of H1975 cells treated with HAD-B1 revealed molecular mechanisms of anti–lung cancer activity of HAD-B1 with increasing p16 and

decreasing pERK1/2 protein expression (Figures 3 and 4). The p16 gene is an important tumor-suppressor gene, involved in the G1 to S phase transition of the cell cycle[30] and regulation of cell cycle progression by inhibiting the S phase.[31] Expression of p16Ink4a maintains the Rb family members in a hypophosphorylated state, which promotes binding to E2F1 and leads to G1 cell cycle arrest.[29] ERK1/2 is serine/threonine protein kinase and member of the mitogen-activated protein kinase family.[32,33] The active ERK1/2 can regulate gene expression, cell proliferation, differentiation, cell matrix interactions, and cell migration, and has been shown to inhibit apoptosis. In contrast, inhibition of ERK1/2 promotes apoptosis.[34,35] Our data showed that the COMTHA appeared to be more effective in suppressing caspase-3, -8, and -9 activities compared with afatinib alone (Figure 7). In addition, the COMTHA-treated cells increased early apoptosis (Figure 5) and G0-G1 phase arrest (Figure 6). These results indicated that upregulation of p16 and downregulation of ERK1/2 in H1975 cells combined treated with the COMTHA resulted in stimulation of caspase-mediated apoptosis and G0-G1 phase cell cycle arrest in the cells.

The tumor growth experiment using H1975 tumor xenograft mice confirmed the synergic effect of combined treatment of HAD-B1 and afatinib. The growth of solid tumor in the COMTHA-treated group was remarkably suppressed in a dose-dependent manner compared with the empty vehicle-treated control groups (Figure 8A). Collectively,
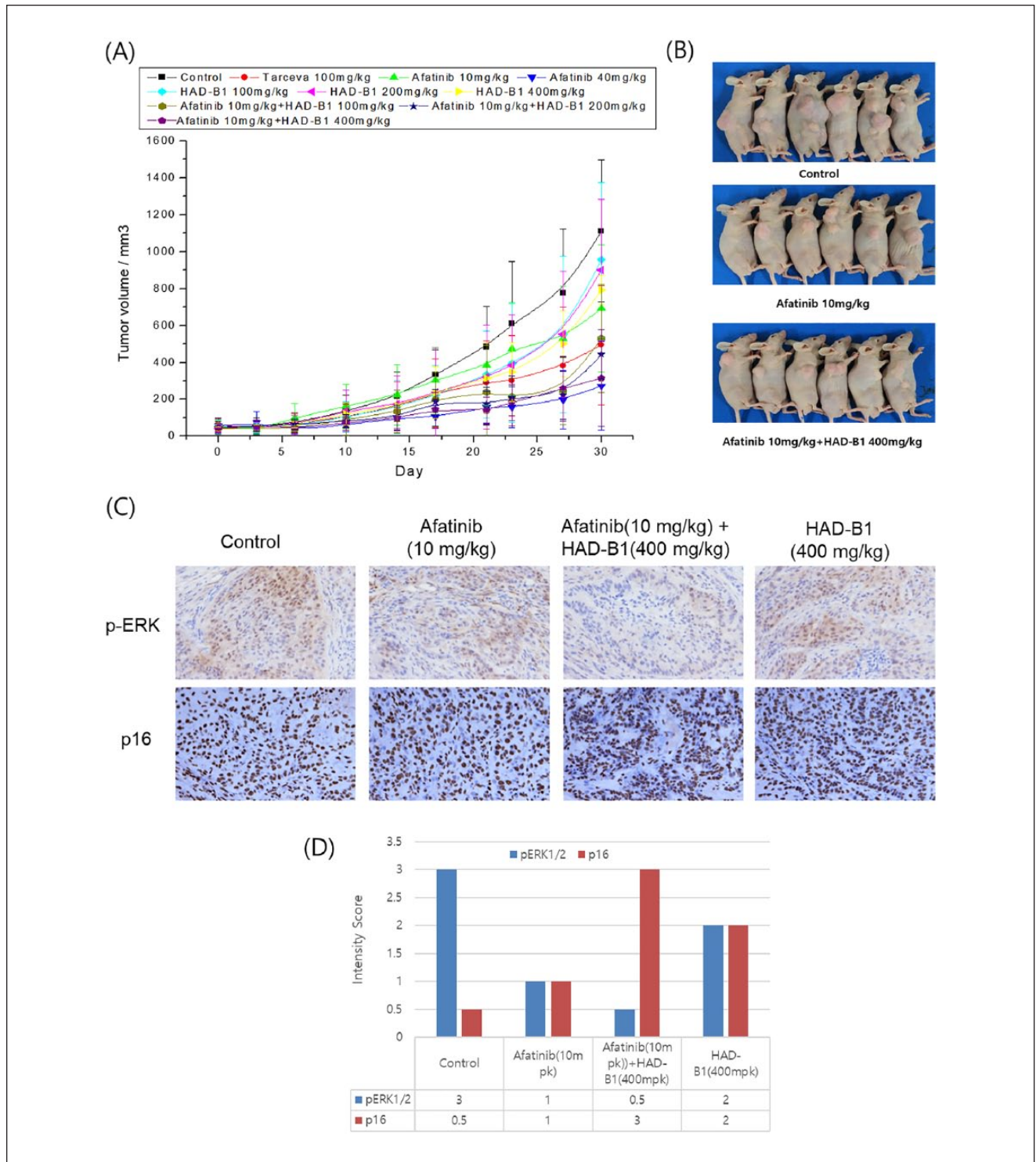
Figure 8. Inhibitory effect of HAD-B1 on solid tumor growth of H1975 lung tumor–cell xenograft animals. H1975 cells (1.0×10^6) were injected subcutaneously into nude mice to generate a xenograft model (n = 8). When tumor growth reached ~100 mm³, HAD-B1 was orally administered at the indicated concentrations for 30 days once daily (A). Representative images of H1975 cells xenograft nude mice treated with the COMTHA (B). Immunohistochemical staining of p-ERK and p16 (C). Quantitative analysis of p16 and pERK1/2 in tumor tissues using the staining intensity score (3, high; 2, middle; 1, low; and 0, control) (D). The images were taken at 400× magnification. Data shown are the means ± SD, and statistical analysis was performed using the Student's *t* test (n = 3; $*P < .05$, $**P < 0.01$, and $***P < .001$, vs control).
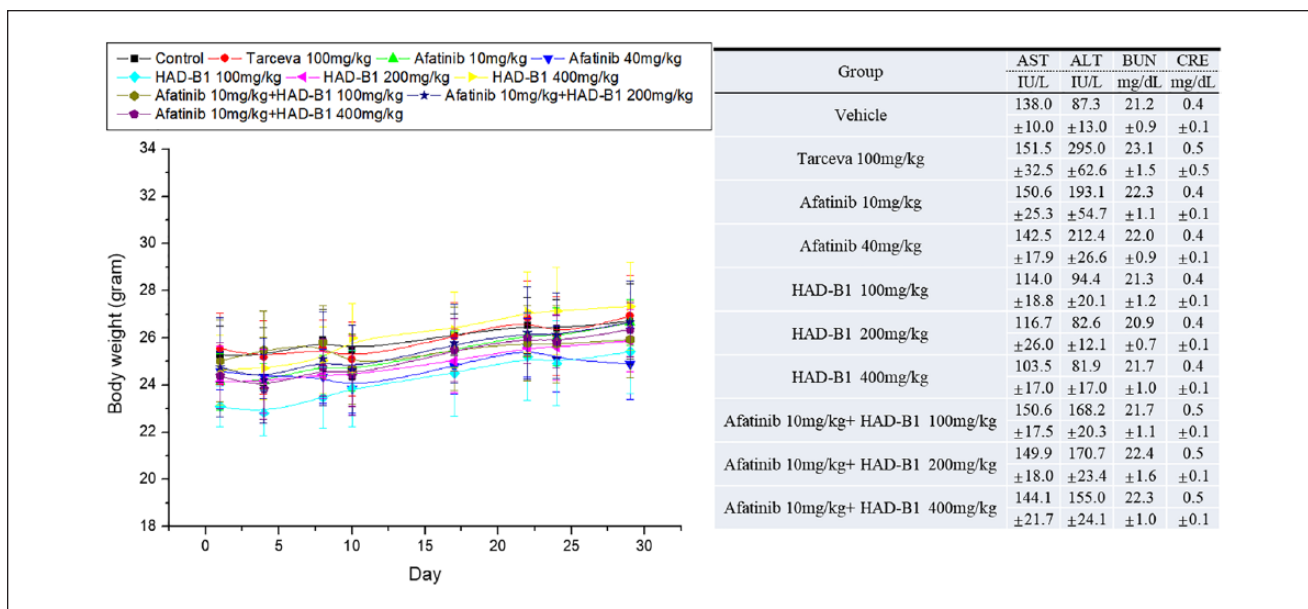
Figure 9. Toxicity analysis in H1975 lung tumor cell–xenograft animals treated with the COMTHA. Body weights (A) and blood chemistry analysis of H1975 tumor-bearing mice (B).

we observed that the COMTHA has an anticancer effect against H1975 lung cancer cells containing EGFR-L858R/ T790M double mutation. Therefore, these findings suggest that HAD-B1 could be an effective and safe drug for treatment of NSCLC patients acquired resistance to TKIs.

Declaration of Conflicting Interests

The author(s) declared no potential conflicts of interest with respect to the research, authorship, and/or publication of this article.

Funding

References

1. Siegel RL, Miller KD, Jemal A. Cancer statistics, 2017. *CA Cancer J Clin*. 2017;67:7-30.
2. Socinski MA, Crowell R, Hensing TE, et al; American College of Chest Physicians. Treatment of non-small cell lung cancer, stage IV: ACCP evidence-based clinical practice guidelines (2nd edition). *Chest*. 2007;132(3 suppl):277S-289S.
3. Boolell V, Alamgeer M, Watkins DN, Ganju V. The evolution of therapies in non-small cell lung cancer. *Cancers (Basel)*. 2015;7:1815-1846.
4. Chan BA, Hughes BG. Targeted therapy for non-small cell lung cancer: current standards and the promise of the future. *Transl Lung Cancer Res*. 2015;4:36-54.
5. Reguart N, Remon J. Common EGFR-mutated subgroups (Del19/L858R) in advanced non-small-cell lung cancer: chasing better outcomes with tyrosine kinase inhibitors. *Future Oncol*. 2015;11:1245-1257.
6. Greenhalgh J, Dwan K, Boland A, et al. First-line treatment of advanced epidermal growth factor receptor (EGFR) mutation positive non-squamous non-small cell lung cancer. *Cochrane Database Syst Rev*. 2016;(5):CD010383.
7. Zhang K, Yuan Q. Current mechanism of acquired resistance to epidermal growth factor receptor-tyrosine kinase inhibitors and updated therapy strategies in human nonsmall cell lung cancer. *J Cancer Res Ther*. 2016;12(suppl):C131-C137.
8. Oxnard GR, Arcila ME, Chmielecki J, Ladanyi M, Miller VA, Pao W. New strategies in overcoming acquired resistance to epidermal growth factor receptor tyrosine kinase inhibitors in lung cancer. *Clin Cancer Res*. 2011;17:5530-5537.
9. Solca F, Dahl G, Zoephel A, et al. Target binding properties and cellular activity of afatinib (BIBW 2992), an irreversible ErbB family blocker. *J Pharmacol Exp Ther*. 2012;343:342-350.
10. Li D, Ambrogio L, Shimamura T, et al. BIBW2992, an irreversible EGFR/HER2 inhibitor highly effective in preclinical lung cancer models. *Oncogene*. 2008;27:4702-4711.
11. Paz-Ares L, Tan EH, O'Byrne K, et al. Afatinib versus gefitinib in patients with EGFR mutation-positive advanced non-small-cell lung cancer: overall survival data from the phase IIb LUX-Lung 7 trial. *Ann Oncol*. 2017;28:270-277.
12. Park K, Tan EH, O'Byrne K, et al. Afatinib versus gefitinib as first-line treatment of patients with EGFR mutation-positive non–small-cell lung cancer (LUX-Lung 7): a phase 2B, open-label, randomised controlled trial. *Lancet Oncol*. 2016;17:577-589.
13. Campo M, Gerber D, Gainor JF, et al. Acquired resistance to first-line afatinib and the challenges of prearranged progression biopsies. *J Thorac Oncol*. 2016;11:2022-2026.

14. Takeda M, Okamoto I, Nakagawa K. Pooled safety analysis of EGFR-TKI treatment for EGFR mutation-positive non-small cell lung cancer. *Lung Cancer*. 2015;88:74-79.

15. Park HR, Lee EJ, Moon SC, et al. Inhibition of lung cancer growth by HangAmDan-B is mediated by macrophage activation to M1 subtype. *Oncol Lett*. 2017;13:2330-2336.

16. Choi YJ, Shin DY, Lee YW, et al. Inhibition of cell motility and invasion by HangAmDan-B in NCI-H460 human non-small cell lung cancer cells. *Oncol Rep*. 2011;26:1601-1608.

17. Bang JY, Kim KS, Kim EY, et al. Anti-angiogenic effects of the water extract of HangAmDan (WEHAD), a Korean traditional medicine. *Sci China Life Sci*. 2011;54:248-254.

18. Li KC, Heo K, Ambade N, et al. Reduced expression of HSP27 following HAD-B treatment is associated with Her2 downregulation in NIH: OVCAR-3 human ovarian cancer cells. *Mol Med Rep*. 2015;12:3787-3794.

19. Kim KH, Kwon YK, Cho CK, et al. Galectin-3-independent down-regulation of GABABR1 due to treatment with Korean herbal extract HAD-B reduces proliferation of human colon cancer cells. *J Pharmacopuncture*. 2012;15:19-30.

20. Kang HJ, Park SJ, Park YM, Yoo HS, Kang IC. Inhibitory effects of HangAmDan–B1 (HAD-B1) on A549 lung cancer cell proliferation and tumor growth in a xenograft model. *Acad J Sci Res*. 2016;4:187-193.

21. Fumagalli S, Totty NF, Hsuan JJ, Courtneidge SA. A target for Src in mitosis. *Nature*. 1994;368:871-874.

22. Chou TC. Drug combination studies and their synergy quantification using the Chou-Talalay method. *Cancer Res*. 2010;70:440-446.

23. Wu GS, Lu JJ, Guo JJ, et al. Synergistic anti-cancer activity of the combination of dihydroartemisinin and doxorubicin in breast cancer cells. *Pharmacol Rep*. 2013;65:453-459.

24. Chen X, Zhu Q, Zhu L, et al. Clinical perspective of afatinib in non-small cell lung cancer. *Lung Cancer*. 2013;81:155-161.

25. Yu X, Ling J, Liu X, et al. Cordycepin induces autophagy-mediated c-FLIPL degradation and leads to apoptosis in human non-small cell lung cancer cells. *Oncotarget*. 2017;8:6691-6699.

26. Lee CY, Hsieh SL, Hsieh S, et al. Inhibition of human colorectal cancer metastasis by notoginsenoside R1, an important compound from *Panax notoginseng. Oncol Rep*. 2017;37:399-407.

27. Lee DG, Jang SI, Kim YR, et al. Anti-proliferative effects of ginsenosides extracted from mountain ginseng on lung cancer. *Chin J Integr Med*. 2016;22:344-352.

28. Khan MA, Ali R, Parveen R, Najmi AK, Ahmad S. Pharmacological evidences for cytotoxic and antitumor properties of boswellic acids from *Boswellia serrata. J Ethnopharmacol*. 2016;191:315-323.

29. Wang Z, Wu X, Liang YN, et al. Cordycepin induces apoptosis and inhibits proliferation of human lung cancer cell line H1975 via inhibiting the phosphorylation of EGFR. *Molecules*. 2016;21:E1267.

30. Ai L, Stephenson KK, Ling W, et al. The p16 (CDKN2a/INK4a) tumor-suppressor gene in head and neck squamous cell carcinoma: a promoter methylation and protein expression study in 100 cases. *Mod Pathol*. 2003;16:944-950.

31. Romagosa C, Simonetti S, López-Vicente L, et al. p16Ink4a overexpression in cancer: a tumor suppressor gene associated with senescence and high-grade tumors. *Oncogene*. 2011;30:2087-2097.

32. Meloche S, Pouysségur J. The ERK1/2 mitogen-activated protein kinase pathway as a master regulator of the G1- to S-phase transition. *Oncogene*. 2007;26:3227-3239.

33. Chambard JC, Lefloch R, Pouysségur J, Lenormand P. ERK implication in cell cycle regulation. *Biochim Biophys Acta*. 2007;1773:1299-1310.

34. Mandal R, Raab M, Matthess Y, Becker S, Knecht R, Strebhardt K. pERK 1/2 inhibit caspase-8 induced apoptosis in cancer cells by phosphorylating it in a cell cycle specific manner. *Mol Oncol*. 2014;8:232-249.

35. Lu Z, Xu S. ERK1/2 MAP kinases in cell survival and apoptosis. *IUBMB Life*. 2006;58:621-631.